Electron drift mobility in a Si-$Ge_{1-x}Si_x$ quantum well at low temperatures

J. Tutor and J. A. Bermúdez
Department of Theoretical Physics, Havana Pedagogical Insitute "E. J. Varona," Ciudad Libertad, Marianao, Havana, Cuba

F. Comas
Department of Theoretical Physics, Havana University, San Lázaro y L, Vedado 10400, Havana, Cuba
(Received 21 August 1991; revised manuscript received 6 March 1992)

The electron drift mobility in a Si-$Ge_{1-x}Si_x$ quantum well at low temperatures is calculated by means of a standard Boltzmann-transport-equation approach in the relaxation-time approximation. Conduction along the Si channel is considered and two scattering mechanisms are discussed: acoustic phonons via deformation-potential coupling and ionized impurities. The role of acoustic phonons is analyzed to be rather important in order to achieve agreement with experimental measurements. All the calculations are done in the quantum size limit and just the first subband is assumed to contribute to electron conduction.

I. INTRODUCTION

Si-$Ge_{1-x}Si_x$ quantum wells (QW's) have been grown along a Si $\langle 001 \rangle$ direction on silicon substrates and with the inclusion of a Ge_ySi_{1-y} buffer layer with a thickness larger than the critical one and therefore relaxed with respect to strains. Intermediate values of y were chosen (for instance $y=0.32$ and $x=0.5$) leading to symmetrically strained structures. In this case strain effects, with a relatively low mismatch at the interfaces, are not very strong. (For a survey on the subject Refs. 1, 2, 3, and 4 are recommended.) Sb donor impurities have been implanted in the $Ge_{1-x}Si_x$ layer by means of a special method called "secondary implantation," with concentrations as high as 5×10^{18} cm^{-3}. Under these conditions, a quasi-two-dimensional (Q2D) electron gas can be formed at the Si layer and considerably high electron mobilities are measured along the Si channel at low temperatures. Although the Si energy gap is wider than that of $Ge_{1-x}Si_x$, a QW is formed for conduction electrons in the Si layer with an energy barrier dependent on the Ge concentration of the buffer layer.

Calculation of the electron drift mobility for conduction along the Si channel in such structures is of obvious importance. In the low-temperature regime, mainly three scattering mechanisms limit the mobility: impurity scattering, surface-roughness scattering, and acoustic-phonon scattering. In Ref. 5, the first two mechanisms were considered in calculations of both the dc and ac conductivity in the $T=0$ limit as a function of electron concentration. In earlier work,[6] we have calculated the electron mobility in a Si-$Ge_{1-x}Si_x$ QW at $T\neq0$, considering only acoustic-phonon scattering [via DP (deformation-potential) coupling]. It should be noted that transport in Si-$Ge_{1-x}Si_x$ structures has also been studied by other authors (see, for example, Refs. 7 and 8), but their calculations were performed on materials with other kinds of energy-band alignment and different doping procedures, while to date the acoustic-phonon scattering mechanism has been included only in Ref. 6.

In Ref. 5, the point was made that surface-roughness scattering mechanism is expected to be of importance for very narrow QW ($d<4$ nm); in the framework of our present calculations, we shall neglect this mechanism and, therefore, we assume our results to be valid for wider QW's ($d\geq10$ nm). In our treatment, a temperature-dependent drift mobility is calculated applying a standard BTE (Boltzman-transport-equation) approach in the relaxation-time approximation. We consider two scattering mechanisms: ionized impurities (both remote and background) and acoustic phonons (via DP coupling). Our calculations made proper use of a Q2D screening factor for impurity scattering. In contrast with our previous calculations of Ref. 6, the electron–acoustic-phonon interaction (via DP coupling) is assumed to be unscreened. This assumption is consistent with the short-range character of the interaction. For the acoustic phonons we made use of a 3D model essentially coincident with the model applied in Ref. 6. However, in the present work we adjusted the bulk values of the phonon parameters (the DP energy and sound velocity) in order to fit experimental values of the mobility. This procedure leads to a temperature-dependent mobility that, at low temperatures ($20<T<150$ K), shows good agreement with experimental data. Consideration of the electron–acoustic-phonon interaction proved to be quite essential for mobility calculations in this temperature range because it is precisely this contribution which reveals a trend in the theoretical curve that is very similar to the experimental result.

Let us summarize the main simplifications made in the present paper.

(i) Electrons are considered to move in a square QW with infinite potential barriers at the interfaces.

(ii) Electron states are calculated in the effective-mass approximation, with neglect of the effects of strain.

(iii) Acoustic phonons are treated in the spirit of the bulk theory and strain effects are also ignored (in neglecting strain effects in both electron states and phonon modes, we introduce a certain error into our model; we expect this error to be small because the actually grown

structures are weakly strained).

(iv) We assume $k_B T \ll E_2 - F$, where E_2 is the bottom energy of the first excited subband, F is the Fermi energy, k_B the Boltzmann constant. Under these conditions, the QSL (quantum size limit) is ensured and we may consider only the first subband to be populated by electrons.

The paper is organized as follows: in Sec. II we calculate the relaxation time for the electron–acoustic-phonon scattering (via DP); in Sec. III the same calculations are made for the case of electron scattering by remote and background ionized impurities; in Sec. IV mobility calculations are presented for different scattering mechanisms; and Sec. V is devoted to the conclusions.

II. RELAXATION TIME: ACOUSTIC-PHONON MECHANISM

Let us take the z axis to be the growth direction with interfaces at $z=0$ and $z=d$. For electron states in the Si layer we apply the effective-mass approximation in close analogy with the approach of Ref. 9, where the Si-SiO_2 inversion layer was discussed (see also Ref. 10). The usual six ellipsoidal energy valleys of bulk Si are reduced to six ellipses of the 2D BZ (Brillouin zone): two of them, corresponding to the lower energies, are two coincident circumferences at the center of the 2D BZ. In the QSL we assume these states to give the main contribution to mobility at low enough temperatures. In other words, in the QSL we suppose that the other energy ellipses are not populated by electrons. More details concerning this approximation can be found in Ref. 6.

Under the above-mentioned assumptions strain effects are neglected. Actually strains should produce energy shifts and other modifications in the energy band structure.

Following similar theoretical assumptions and calculations done in our previous work[6] for electron wave function and the corresponding electron energies, and using the momentum relaxation time according to the standard BTE approach in the QSL regime, one obtains

$$\frac{1}{\tau_{\rm ph}} = \frac{3\pi m_t k_B T}{2\hbar^3 \rho d} \frac{\Xi^2}{s_l^2} , \tag{1}$$

valid for intrasubband electron scattering in the first subband. In Eq. (1) m_t is the transverse effective mass here referred to the direction perpendicular to [001] of bulk Si. Also, in (1), Ξ is defined by

$$\Xi = \Xi_l + \tfrac{1}{3}\Xi_t , \tag{2}$$

where Ξ_l and Ξ_t are quantities related to the deformation-potential energy in the longitudinal and transverse directions; and s_l is the longitudinal sound velocity.

Let us now point out that in Ref. 6 a more complicated expression for $\tau_{\rm ph}$ was obtained because the interaction was assumed to be screened. As remarked in Sec. I, here we neglect screening for a short-ranged interaction, as is the case of electron–acoustic-phonon coupling (via DP).

In Eq. (1) strain effects are neglected. For sufficiently weak strains, Eq. (1) is expected to be essentially correct but some parameters (for instance, Ξ and s_l) may have to be adjusted. This idea was actually implemented in the numerical calculations and a comparison with experimental measurements was made. Of course, a more rigorous approach to this problem requires one to consider strain for both the electron states and phonon modes.

III. RELAXATION TIME: IMPURITY-SCATTERING MECHANISM

In the case of electron scattering by ionized impurities, we follow a treatment approximately along the lines of Ref. 11, which gives us the relaxation time

$$\frac{1}{\tau_i(E)} = \frac{e^4}{4\pi\epsilon_0^2\kappa^2\hbar E}\int_0^{\pi/2}\frac{\Gamma(Q)}{\epsilon^2(Q)}d\alpha , \tag{3}$$

where the relaxation time for the impurities $\tau_i(E)$ is explicitly dependent on the parameter $E=\hbar^2k^2/2m_t$ and

$$Q^2 = \frac{8\pi m_t E}{\hbar^2}\sin^2\alpha . \tag{4}$$

The function $\Gamma(Q)$ is defined by

$$\Gamma(Q) = \int_{-\infty}^{\infty} dz_0 N_I(z_0)|G(Q,z_0)|^2 . \tag{5}$$

In Eq. (5), $N_I(z_0)$ is the volume concentration of impurities as a function of z_0, assuming ionized impurities at positions (x_0,y_0,z_0). This approach is quite standard for dilute impurities distributed at random. $G(Q,z_0)$ is defined as

$$G(\mathbf{Q},z_0) = \int_0^d |\varphi(z)|^2 e^{-Q|z-z_0|}dz , \tag{6}$$

where $\varphi(z)$ is the part of the electron wave function in the confinement direction as was used by the authors in Ref. 12.

In Eq. (3) ϵ_0 is the free-space permittivity [in Système International (SI) units] and κ is the dielectric constant, which, for a Si_xGe_{1-x} alloy, is given by

$$\kappa(x) = 11.7 + 2.25(1-x) . \tag{7}$$

As usually done in this kind of problem, it is assumed that the layered structure has an almost uniform dielectric constant, which can be determined from Eq. (7), fixing a unique value of x for all layers or taking some kind of average value. In our numerical calculations we take $x=1$.

According the Ref. 9 we defined the Q2D dielectric function $\epsilon(Q)$ by the formula

$$\epsilon(Q) = 1 - \frac{e^2}{2\epsilon_0\kappa Q} g(Q)\Pi(Q) , \tag{8}$$

where

$$g(Q) = \int dz \int dz' |\varphi(z)|^2 |\varphi(z')|^2 e^{-Q|z-z'|} \tag{9}$$

is a form factor taking into account the finite extension (into the z direction) of the Q2D wave function. It can be easily proved that

$$g(x)=\frac{2}{x}+\frac{x}{x^2+4\pi^2}-\frac{32\pi^4(1-e^{-x})}{(x^2+4\pi^2)^2x^2}\ , \tag{10}$$

with $x=Qd$. The temperature-dependent polarization factor $\Pi(Q,T)$ is in general defined by means of

$$\Pi(Q,T)=\frac{4m_t}{\hbar^2 S}\sum_{\mathbf{k}}\frac{f_0(\mathbf{k}+\mathbf{Q})-f_0(\mathbf{k})}{(\mathbf{k}+\mathbf{Q})^2-\mathbf{k}^2}\ . \tag{11}$$

In Eq. (11) we introduced the standard equilibrium Fermi Dirac distribution function f_0, where E is defined after Eq. (3) and F is the Fermi energy.

For $T=0$ it can be shown that (see Refs. 10 and 11)

$$\Pi(Q)=\frac{m_t}{\pi\hbar^2}\left\{\left[1-\frac{4}{Q^2}(k_F-k_1)^2\right]^{1/2}\times\Theta(Q-2(k_F-k_1))-1\right\}\ , \tag{12}$$

where

$$k_F=\left[\frac{2m_tF}{\hbar^2}\right]^{1/2},\quad k_1=\left[\frac{2m_tE_1}{\hbar^2}\right]^{1/2},$$

and $\Theta(x)$ is the step function. For $T\neq 0$ there is not an explicit analytical expression for $\Pi(Q,T)$. As discussed in Ref. 13 (see also Ref. 10) we can use an approximate generalization of $\Pi(Q)$ to the finite temperature case in the form

$$\Pi(Q,T)=\int_0^\infty\frac{\Pi(Q,F_1')dF_1'}{4k_BT\cosh^2\left[\frac{F_1-F_1'}{k_BT}\right]}\ , \tag{13}$$

where $\Pi(Q,F_1')$ means we evaluate Eq. (12) for a given Fermi energy F_1' and then integrate over F_1' according to Eq. (13). In our case we use $F_1'=F'-E_1$.

Concerning the impurity distribution we made the following assumptions (closely related with the situation depicted in Ref. 3). For background impurities,

$$N_i(z_0)=\begin{cases}N_B & \text{if } 0\le z_0\le d\\ 0 & \text{otherwise}\ .\end{cases} \tag{14}$$

For remote impurities,

$$N_i(z_0)=\begin{cases}N_R & \text{if } -b-a\le z_0\le -b;d+b\le z_0\le d+b+a\\ 0 & \text{otherwise}\ .\end{cases} \tag{15}$$

N_B and N_R are two constants that should be taken from experiment. b and a are the spacer and remote impurity layer thicknesses, respectively. Substitution of Eqs. (14) and (15) into Eq. (5) gives

$$\Gamma(x)=\frac{16\pi^4 d}{(x^2+4\pi^2)^2x^2}\left\{4N_B\left[1+\frac{x^2}{2\pi^2}+\frac{3x^4}{32\pi^4}+\tfrac{1}{2}e^{-x}+\frac{(1-e^{-2x})}{4x}+\frac{4(e^{-x}-1)(x^2+2\pi^2)}{(x^2+4\pi^2)x}\right]+N_R\frac{e^{-2\xi x}(1-e^{-x})^2}{x}(1-e^{-2\eta x})\right\}, \tag{16}$$

where $x=Qd$, $\xi=b/d$, $\eta=a/d$. Using Eqs. (16) and (8) in Eq. (3), we determine $\tau_i(E)$, a complicated function of E which should be handled numerically.

IV. MOBILITY CALCULATION

Mobility can be calculated according to the following expression:

$$\mu(T)=\frac{4e}{\pi\hbar^2 n_s}\int_0^\infty\tau(E)[-f_0'(E)]E\,dE\ , \tag{17}$$

where

$$\frac{1}{\tau(E)}=\frac{1}{\tau_{\rm ph}}+\frac{1}{\tau_i(E)} \tag{18}$$

and

$$n_s=\frac{2m_tk_BT}{\pi\hbar^2}\ln(1+e^{F_1/k_BT})\ , \tag{19}$$

is the areal electron concentration in the Si channel. All the above formulas are valid in the QSL when just the first subband is populated. A factor of 2 was also included because at the BZ center we have two coincident energy circumferences contributing to conduction.

Another important point to be remarked is that we are fixing the Fermi level F (or $F_1=F-E_1$) assuming there is an infinite reservoir of electrons (in the SB-doped sheets). Then $n_s=n_s(T)$ is a function of temperature. In our calculations F is fixed in a somewhat arbitrary way in the form $F\cong E_1$ in order to ensure the QSL.

V. CONCLUSIONS

Equation (17) for the drift mobility corresponds to the approximations discussed throughout the paper and summarized in Sec. I. Applying this equation we have found mobility as a function of temperature.

For numerical computations we use QW parameters from Ref. 3: $b=10$ nm, $a=5$ nm, $d=10$ nm, $N_R=5\times10^{24}$ m^{-3}; electron effective masses were taken the same as in the bulk case: $m_l=0.92m_0$ and

$m_t = 0.19 m_0$. For the static dielectric constant we set $\kappa = 11.70$ (Si dielectric constant).

Concerning parameters ρs_l^2 and Ξ, we apply the following procedure:

$$\Xi^2/\rho s_l^2 = \beta^2 \frac{\Xi_b^2}{(\rho s_l^2)_b} , \tag{20}$$

where β is a fitting parameter and $\Xi_b = 6.5$ eV according to the reported bulk value of Ref. 14, while $(\rho s_l^2)_b = 1.67 \times 10^{11}$ N/m^3 from Ref. 15. Parameter β was adjusted in order to fit the experimental value of μ for $T = 100$ K, once the Fermi energy F was fixed. The Fermi energy F is assumed fixed in our calculations (as discussed above) and was chosen in a somewhat arbitrary way which ensures the QSL approximation, i.e., F is chosen nearly above (or equal to) E_1 but below E_2; therefore $E_2 - F \gg k_B T$ for low enough temperatures. We suppose this approach is the better one insofar as we do not have enough information for an *a priori* determination of F from experiment.

Of course, the above-mentioned procedure enables us to get a certain estimation of $\Xi^2/\rho s_l^2$ for our case, provided that our model for acoustic phonons [see Eq. (1)] is good enough. In principle the effective masses m_l and m_t should also be adjusted. All those parameters must be modified by the strains. However, our parametrization of the electron-phonon contribution to mobility leads to a close agreement with the experimental curve.

In Fig. 1 we show $\log_{10}\mu$ vs T for fixed values of the other parameters and $F = 4.2$ meV, $N_B = 10^{21}$ m^{-3}. The different scattering mechanisms are presented separately: the curve with triangles is the phonon contribution, the curve with # represents the remote-impurity contribution, and the curve with ◇ gives the background-impurity contribution. The curve with squares gives the total mobility including all the above-mentioned mechanisms, while the curve with crosses is the experimental curve from Ref. 3. We note that the phonon contribution is important for temperatures above $T = 20$ K and produces a trend analogous to the experimental curve. This latter fact proves that the electron-phonon scattering mechanism cannot be neglected for temperatures above 20 K in the description of mobility curves. It should be remarked that experimental results from Ref. 3 are concerned with Hall mobilities, which are approximately equal to the drift mobilities we have calculated (up to a factor of order 1). All parameters were taken from Ref. 3 except N_B which was adjusted in order to achieve better agreement with experiment.

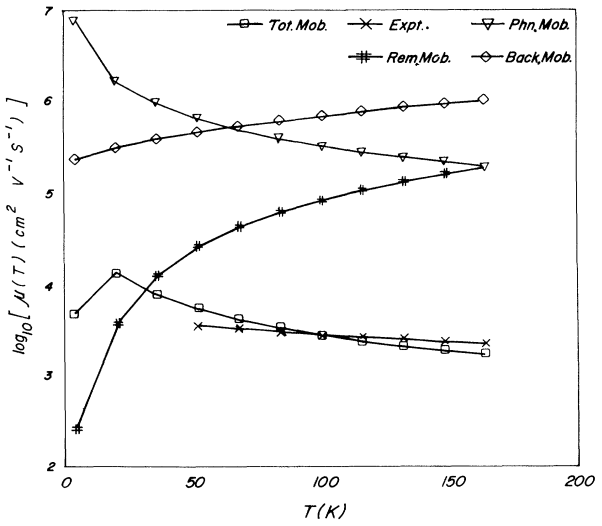

FIG. 1. Mobility logarithm vs temperature of the 2DEG in a Si-$Si_{0.5}Ge_{0.5}$ QW structure for different scattering mechanisms: phonon contribution, remote-impurity contribution, and background-impurity contribution. Also presented are total mobility and experimental mobility from Ref. 3. QW parameters are well width $d = 10$ nm; spacer $b = 10$ nm; remote-impurity-layer thickness $a = 5$ nm; remote-impurity concentration $N_R = 5 \times 10^{24}$ m^{-3}; background-impurity concentration $N_B = 10^{21}$ m^{-3}; and Fermi level $F = 4.2$ meV. The adjustable parameter β was taken to be 4.11.

In our calculations we have taken a value of F ensuring the QSL, in contrast with the value assumed in Table I of Ref. 3 for sample C273, the case which we have used for comparison. It must be remarked that in the above-mentioned reference, F was not measured but calculated in the $T = 0$ K approximation. This latter calculation, in our opinion, was not quite rigorous.

In all our figures mobility was expressed in usual units (cm^2/V s). In Fig. 2 we show μ vs T just for total mobility and the experimental result from Ref. 3. In this figure the same parameters were taken and it can be clearly seen that an acceptable agreement with experiment has been found. As can be seen, a relatively large mobility is predicted by us at very low temperatures ($\cong 20$ K). In our calculations, besides the various approximations that we have already discussed in the paper, we only considered two scattering mechanisms. However, a very acceptable

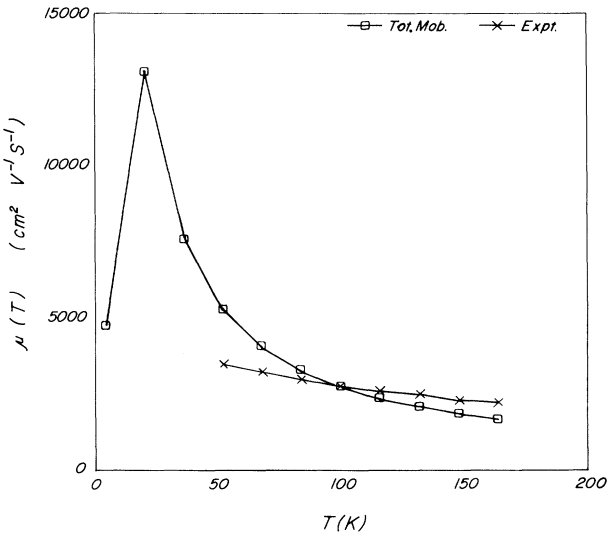

FIG. 2. Temperature-dependent total mobility of the 2DEG in a Si-$Si_{0.5}Ge_{0.5}$ QW. Experimental results from Ref. 3 are also included. QW parameters and the adjustable parameter β are the same as in Fig. 1.

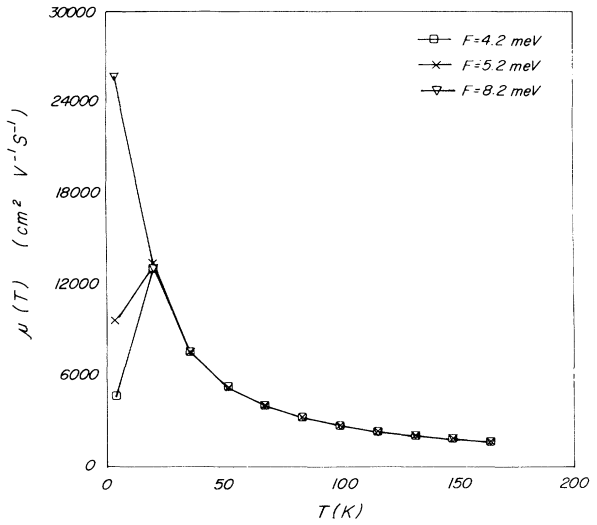

FIG. 3. Temperature-dependent total mobility is shown for the same parameters as in Fig. 1, except Fermi level F. The Fermi level was set equal to $F=4.2$, 5.2, and 8.2 meV.

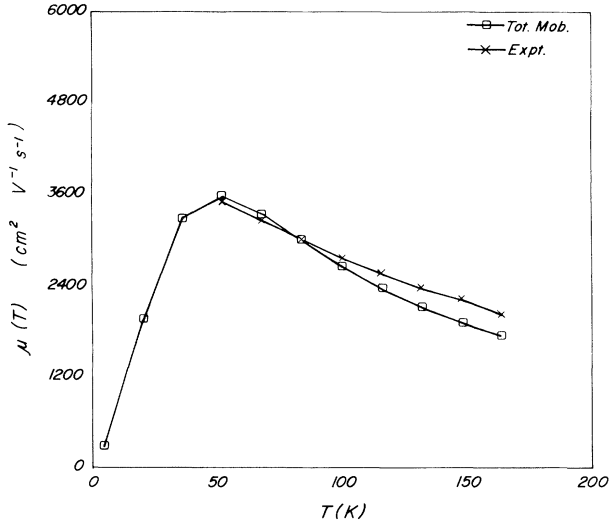

FIG. 4. Total mobility vs temperature is shown as well as the experimental result from Ref. 3. All parameters were chosen as in Fig. 1 except that $N_B=4\times10^{23}$ m^{-3}.

agreement with experiment is obtained as indication that we have studied the fundamental scattering mechanisms in the selected range of temperature.

In Fig. 3 we show μ vs T for total mobility. The parameters were the same as in previous figures except for F, which was set equal to $F=4.2$, 5.2, and 8.2 meV. As can be observed, at temperatures above $T=20$ K, these three curves coincide. For $T<20$ K, increasing mobility is observed only for $F=8.2$ meV, and it is seen that the phonon mechanism is dominant; for lower values of F, mobility is dominated by the impurity mechanism. For increasing values of F, it is seen that the phonon mechanism is dominant (but a departure from the QSL approximation is slightly higher). Neither in the experimental results (Ref. 3), nor in our calculations, can the value of the Fermi energy be rigorously determined.

In Fig. 4 we show μ vs T for total mobility and the experimental result. This case is rather curious because a very good agreement between our theoretical result and experiment is achieved when we choose all parameters as in Fig. 1 but with $N_B=4\times10^{23}$ m^{-3}. In Ref. 3, the value of N_B was not reported. Because of the approximations done in our calculations this latter result is merely a curiosity, and such a large value of N_B cannot be taken as correct.

Our calculations were done on the basis of a simple model. In order to get more accurate results, the following should be taken into account: a more detailed solution of the Boltzmann equation including intersubband processes, i.e., an approximation better than the QSL; a more realistic consideration of electron states and phonon modes for strained structures.

Nevertheless, within our approximations we were able to obtain acceptable results that prove the relative importance of the phonon scattering mechanism in the range of temperatures considered. In the current paper we also included impurity scattering, as did Gold in Ref. 5. In all previous works, including that of Gold, phonons were not considered. However, we have proved that phonon contribution is essential even at low temperatures for reproduction of the experimental curves.

[1]E. Kasper, H. J. Herzog, H. Jorke, and G. Abstreiter, Superlatt. Microstruct. **3**, 141 (1987).
[2]H. Jorke and H. J. Herzog, J. Electrochem. Soc. **133**, 989 (1986).
[3]H. J. Herzog, H. Jorke, and F. Schöfler, Thin Solid Films **184**, 237 (1990).
[4]G. Abstreiter, H. Brugger, T. Wolf, R. Zchai, and Ch. Zeller, in *Two-dimensional Systems: Physics and New Devices,* Proceedings of the International Winter School, Mantendorf, 1986, edited by G. Bauer, F. Kuchar, and H. Heinrich (Springer-Verlag, Berlin, 1986), p. 130.
[5]A. Gold, Phys. Rev. B **35**, 723 (1987).
[6]J. Tutor, J. A. Bermúdez, and F. Comas, Phys. Status Solidi B **163**, 125 (1991).
[7]J. A. Moriarty and S. Krishnamurthy, J. Appl. Phys. **54**, 1892 (1983).
[8]S. Krishnamurthy and J. A. Moriarty, Phys. Rev. B **32**, 1027 (1985).
[9]F. Stern and W. E. Howard, Phys. Rev. **163**, 816 (1967).
[10]T. Ando, A. B. Fowler, and F. Stern, Rev. Mod. Phys. **54**, 437 (1982).
[11]G. Bastard, *Wave Mechanics Applied to Semiconductor Heterostructures* (Les Editions de Physique, 1989), Chap. VI.
[12]J. Tutor, J. A. Bermúdez, and F. Comas (unpublished).
[13]P. F. Maldague, Surf. Sci. **73**, 296 (1978).
[14]K. Hess, Appl. Phys. Lett. **35**, 484 (1974).
[15]D. L. Rode, Phys. Status Solidi B **53**, 245 (1972).